



Sonographic Evaluation of the Shoulder

3

Avner Yemin and Ronald S. Adler

3.1 Introduction

Diagnostic shoulder sonography has been well documented and established as an accurate tool for evaluation of shoulder pathology. In fact a meta-analysis study has shown the sensitivity and specificity of diagnostic ultrasound to be comparable to those of conventional MRI [1]. However, the diagnostic accuracy of shoulder sonography has been shown to depend on the experience and skill of the sonographer [2]. Although shoulder sonography may be time consuming for the novice, with experience, a better understanding of the sonographic anatomy, and the use of a standardized protocol, the examination can be performed quickly [3]. In addition to its short acquisition time, shoulder sonography has a marketable advantage of being inexpensive when compared to MRI. However, the most distinct advantage is the ability to assess for pathology in real time both at static and dynamic states. Provocative maneuvers can be performed to assess for pathology amenable to be accentuated by positional maneuvers, for example,

impingement syndromes [4]. In addition to gray-scale imaging the use of color and/or power Doppler imaging can be utilized to detect hyperemia during the examination, which has been associated with symptomatic tendinopathy, inflammation, and repair states. In this chapter we discuss the approach to performing shoulder sonography, relevant anatomy, and relevant interpretation pitfalls.

3.2 Sonographic Shoulder Anatomy

There are four muscles and tendons, which make up the rotator cuff: the supraspinatus, the infraspinatus, the subscapularis, and the teres minor. Normal muscle on sonography appears as a structure made up of a hypoechoic background with superimposition of multiple curvilinear and sometimes punctate echogenic areas corresponding to the perimysial connective tissue (Figs. 3.1 and 3.2).

The four tendons of the rotator cuff each has unique bony attachments, which are used as landmarks to assist in identification of each tendon. The supraspinatus tendon inserts onto the superior facet and superior half of the middle facet of the greater tuberosity. The infraspinatus tendon also inserts along the middle facet of the greater tuberosity, just posterior to the supraspinatus tendon and with some overlap of the fibers in a junctional zone. The teres minor

A. Yemin (✉)
Envision Physician Services—Radiology Associates
of Hollywood, Memorial Healthcare System,
Hollywood, FL, USA
e-mail: avner.yemin@shcr.com

R. S. Adler
Department of Radiology, NYU Langone Health,
New York, NY, USA
e-mail: Ronald.Adler@nyulangone.org

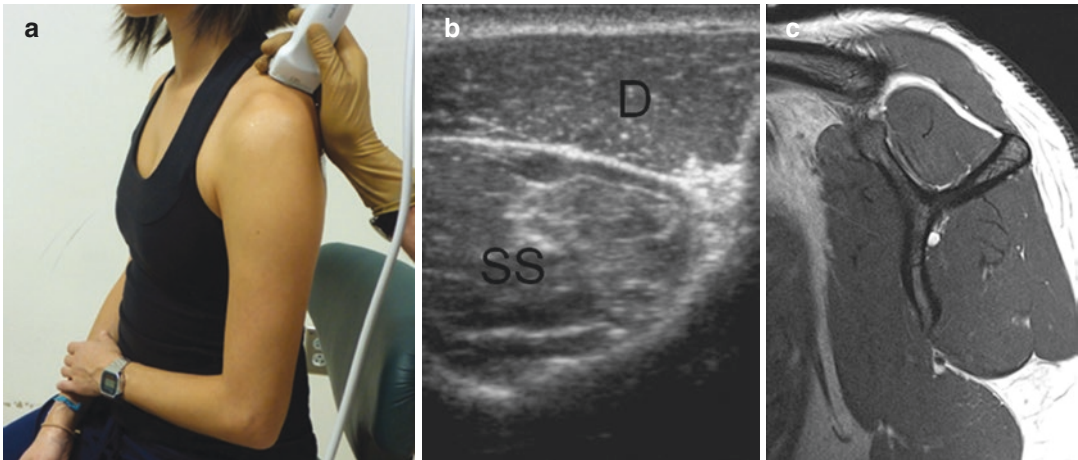


Fig. 3.1 Muscle imaging—supraspinatus patient positioning (a); short-axis sonographic image (b); MRI correlate (c); supraspinatus (SS); deltoid (D)

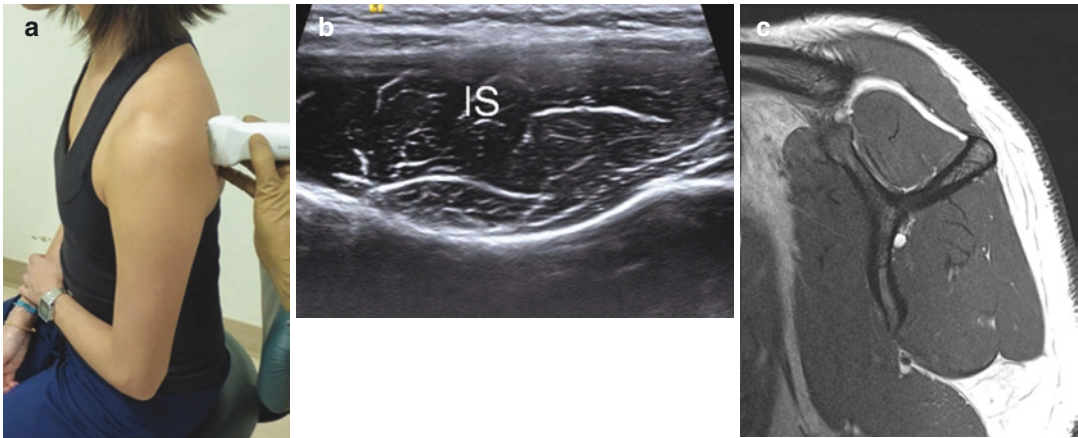


Fig. 3.2 Muscle imaging—infraspinatus patient positioning (a); short-axis sonographic image (b); MRI correlate (c); infraspinatus (IS)

tendon is positioned inferior to the infraspinatus tendon and thus inserts along the inferior facet of the greater tuberosity [5]. The subscapularis tendon inserts onto the lesser tuberosity of the humerus.

As demonstrated in Fig. 3.3, deep to the subdeltoid bursa is the supraspinatus tendon, which is a convex echogenic structure with well-demarcated convex margin that tapers distally as it inserts on the footprint. It is crucial to be able to distinguish the thin hypoechoic area, which is often seen as the tendon fiber insert, from a partial-thickness tear or tendinosis.

The long head of the biceps tendon has both intra- and extra-articular components. It

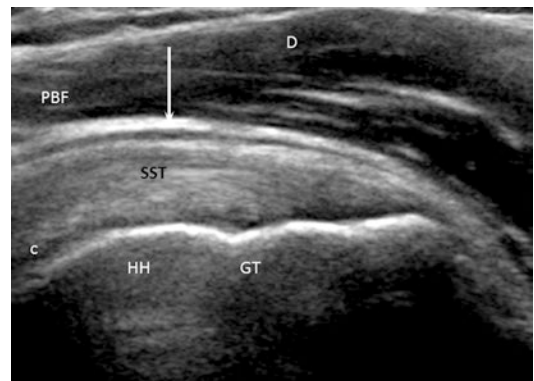


Fig. 3.3 Supraspinatus long-axis view—supraspinatus tendon (SST); deltoid (D); peri-bursal fat (PBF); subdeltoid bursa (arrow); convex tendon (c); greater tuberosity (GT); humeral head (HH)

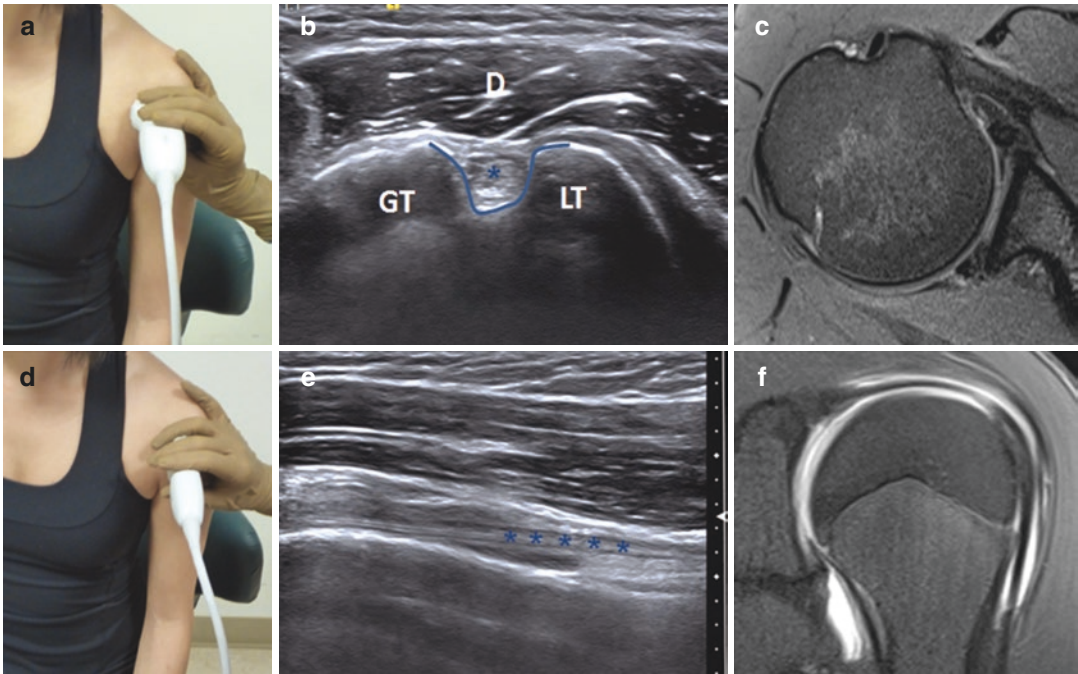


Fig. 3.4 Biceps tendon—short-axis patient positioning (a); short-axis sonographic image (b); MR correlate of short axis (c); long-axis patient positioning (d); long-axis

sonographic image (e); MR correlate of long axis (f); biceps tendon (*) Greater tuberosity (GT); lesser tuberosity (LT); Biceps groove (curved line)

originates from the superior margin of the glenoid and courses anterolaterally through the rotator interval and extends inferiorly between the greater and lesser tuberosities in the bicipital groove (a.k.a. intertubercular groove), where it is considered extra-articular (Fig. 3.4).

The subacromial-subdeltoid bursa is a synovial lined space that lies deep to the deltoid and acromion. As demonstrated in Fig. 3.3, there is a distinct peri-bursal fat stripe deep to the deltoid. The subdeltoid bursa is interposed between the fat stripe and the superficial margin of the tendon and is generally seen as a thin hypoechoic line, usually less than 2 mm in thickness in normal individuals [3]. This can be distended in the setting of subacromial/subdeltoid bursitis.

3.3 Nomenclature

When performing ultrasound the orientation of the transducer is positioned in multiple different planes as we attempt to best view the tendons.

Additionally certain positions are used to optimally view the different tendons creating oblique views. Therefore utilizing the standard anatomic planes for sonography can create confusion. As such it is convenient to discuss tendons in terms of long axis or short axis. The long-axis view assesses the tendon in length as it attaches on the footprint and the short-axis view is perpendicular to that (Fig. 3.5).

3.4 Anisotropy

The difficulty with scanning the shoulder in particular is that the structures are curvilinear which leads to issues with anisotropy so that when you are scanning initially the most echogenic portion is going to be that portion of the tendon which is perpendicular to the transducer scan plane. However, if the adjacent tendon fibers are angled, and not perpendicular to the transducer, the tendon will appear progressively hypoechoic due to anisotropy, which can easily be mistaken for tendinosis or tear. This problem

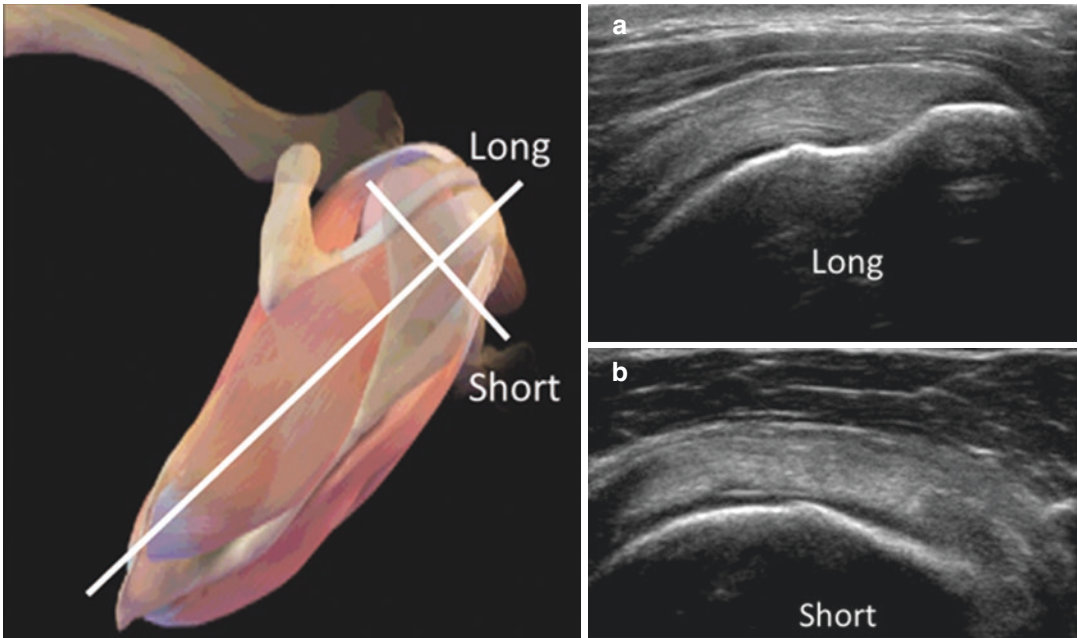


Fig. 3.5 Tendon orientation—long-axis (a) and short-axis (b) views

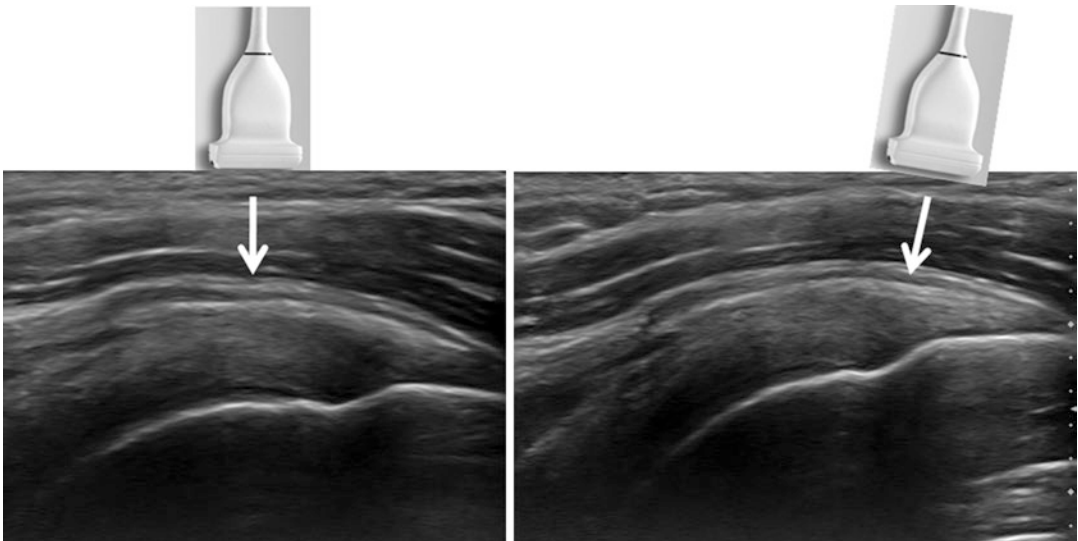


Fig. 3.6 Rocking the transducer to eliminate anisotropic effect at footprint

is very common, as an angle of as little as $2\text{--}3^\circ$ has been shown to produce anisotropy [6]. Hence, when scanning, it is critical to reorient the transducer so that it is perpendicular to the tendon fibers being evaluated to exclude anisotropy for the hypoechoic nature of the tendon.

This anisotropy is commonly seen at the tendon footprint where the tendon fibers are curvilinear as they attach to bone. Rocking of the transducer back and forth along the long axis can be used to show if there is a true tear or just anisotropy (Fig. 3.6).

Table 3.1 Standardized shoulder sonography protocol

| | | |
|---|--|---|
| Biceps | Short axis—3 images → proximal to distal | Long axis—2 images → proximal and distal |
| AC joint | 1 image across joint | |
| Subscapularis | Short axis—3 images → near coracoid, mid, and distal | Long axis—2 images → proximal and distal |
| Muscle – Infraspinatus – Teres minor – Supraspinatus | Short axis only 1 image each | |
| Supraspinatus/infraspinatus (Crass or modified Crass) | Short axis—3 images → proximal to distal | Long axis—3 images → lateral (infraspinatus), mid (junctional zone), medial (near rotator interval) |

3.5 Technique

Several different guidelines have been established for performance of shoulder sonography, some of which advocate that the sonographer is positioned in front of the patient and others advocate scanning from behind the patient [6–8]. We have found approaching the patient from the front to be most convenient and for the purposes of the chapter will be describing this technique. We advise having the patient sitting down on a chair, which can revolve to ease the transitions between steps. In addition patient positioning should be optimized to allow for the most ergonomically comfortable scanning position for the examiner.

The two most important aspect of shoulder sonography is to maintain a standardized protocol with a systematic approach and second is to properly position the arm to optimally look at all the shoulder structures (Table 3.1). We advise looking at the anterior structures first followed by posterior structures and lastly evaluating the supraspinatus tendon, as the positioning is usually the most uncomfortable for the patient, thus leaving the worst for last.

3.6 Step-by-Step Guideline

3.6.1 Step 1: Evaluating the Long Head of the Biceps Tendon (Fig. 3.4; Table 3.2)

The patient should be seated with the arm at their side with the elbow in 90-degree flexion and the

Table 3.2 Biceps tendon guidelines

| | Technique | Findings |
|------------------|---|--|
| Short axis first | – One image above groove – At least 2 below | – Tendon is an echogenic ellipse in the bicipital groove – Demonstrates fluid/synovitis |
| Long axis | – Turn transducer 90° – To avoid anisotropy tilt transducer to maximize echogenicity | Tendon is linear and fibrillar |

forearm supinated. This position places the bicipital groove anteriorly. In short axis you should see the long head of the biceps tendon within the bicipital groove. By turning the transducer 90° you can assess the length of the long head of the biceps tendon as an echogenic fibrillar structure. In certain situations you may need to rock the transducer back and forth in order to make the transducer as parallel to the biceps tendon as possible.

3.6.2 Step 2: Evaluating the Acromioclavicular Joint (Fig. 3.7)

Start by palpating the acromioclavicular joint and placing the transducer in long axis along the top of the joint. You will be able to see the distal clavicle and acromion and the interposed joint capsule/fibrocartilage disc. When assessing the acromioclavicular joint look for joint capsular distension, osseous irregularities, joint widening, or a step-off between the clavicle and acromial process. If there is suspicion for a widened joint

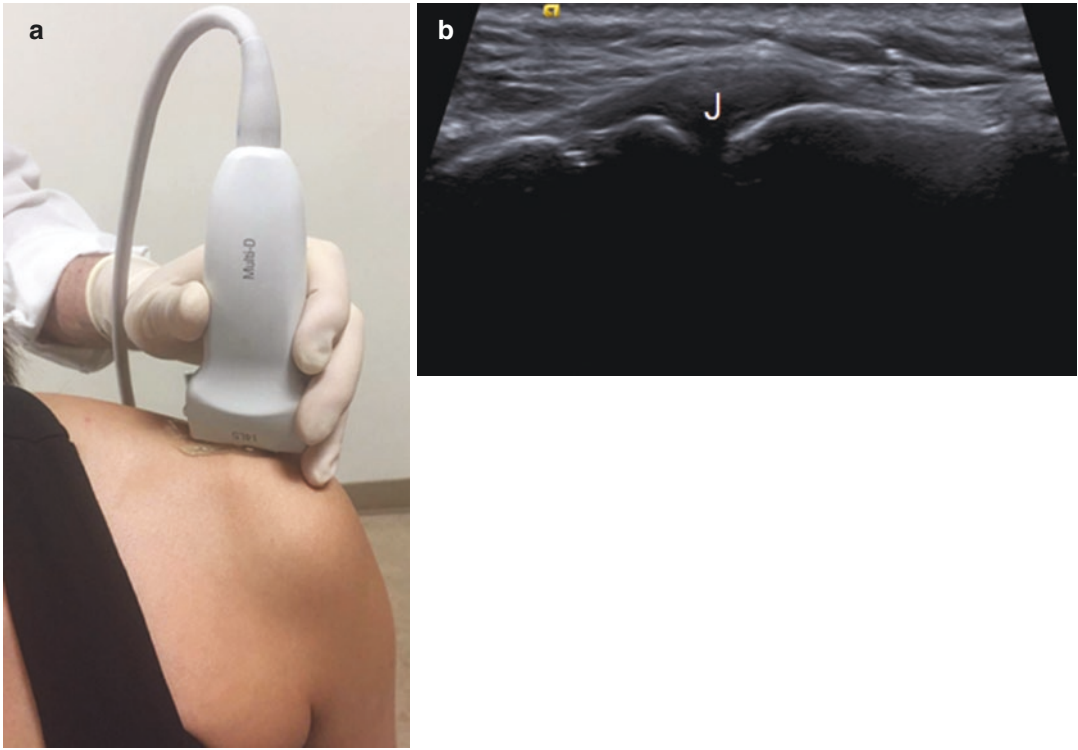


Fig. 3.7 Acromioclavicular joint imaging—patient positioning (a); sonographic image (b); joint capsule (J)

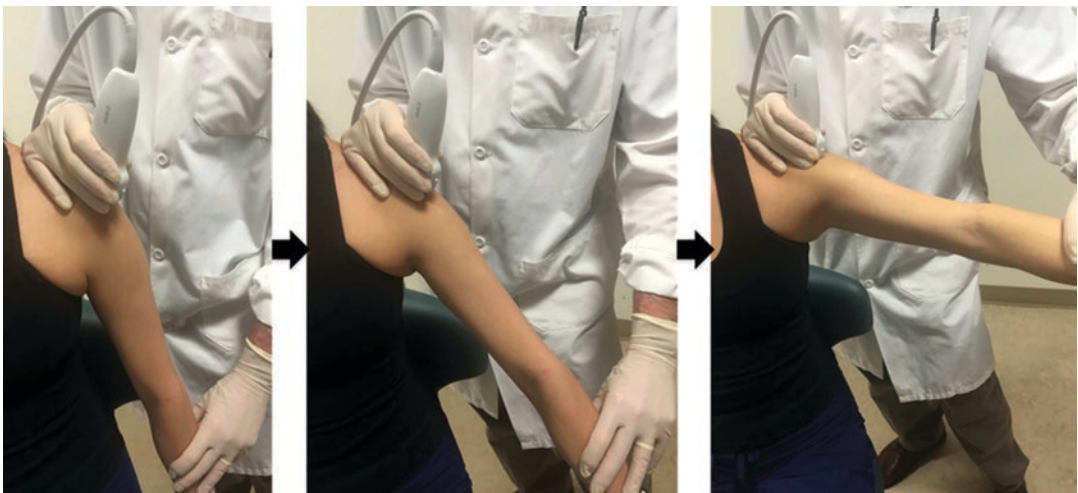


Fig. 3.8 Subacromial impingement dynamic imaging—patient positioning with progressive increase of arm abduction while imaging

or articular step-off dynamic maneuvers such as internally and externally rotating the patient's arm actively can be utilized.

Additionally dynamic maneuvers can be performed to assess for subacromial impinge-

ment (Fig. 3.8). This is done by placing the transducer just lateral to the acromial process and moving the patient's arm through a range of abduction and adduction while imaging. Findings of subacromial impingement include

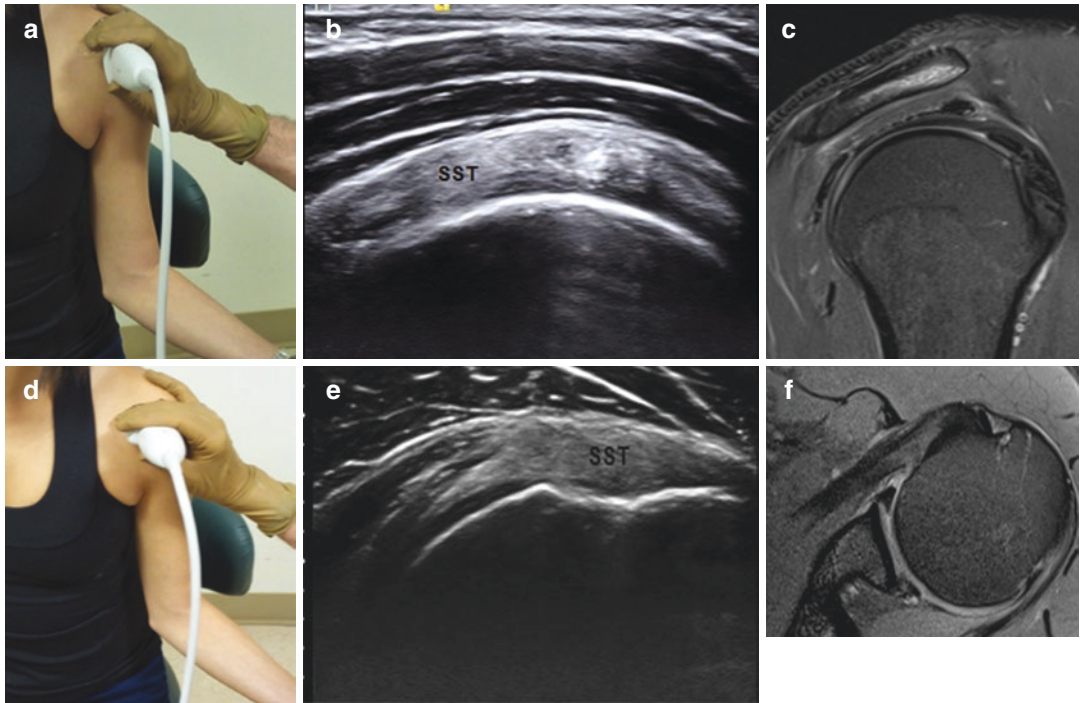


Fig. 3.9 Subscapularis tendon—short-axis patient positioning (a); short-axis sonographic image (b); MR correlate of short axis—multipennate (c); long-axis patient

positioning (d); long-axis sonographic image (e); MR correlate of long axis (f); supraspinatus tendon (SST)

snapping of the bursal tissue and abnormal upward migration of the humeral head with respect to the acromion [8].

3.6.3 Step 3: Subscapularis Tendon
(Fig. 3.9; Table 3.3)

The patient’s arm should be placed in external rotation in order to bring the subscapularis away from the coracoid process which otherwise would partially impede visualization due to dense shadowing. External rotation will therefore expose the subscapularis tendon and place it in some degree of hyperextension. The footprint of the subscapularis tendon will be seen as a curvilinear structure tapering down to the bony attachment. Assessment of the subscapularis footprint is achieved by looking at the anatomic neck and the beginning of the humeral head articular cartilage (black line). As discussed in the nomenclature section, the long-axis view is in respect to the

Table 3.3 Subscapularis tendon

| | Technique | Findings |
|-----------------------|---|---|
| Long-axis image first | Externally rotate forearm with transducer in fixed position | <ul style="list-style-type: none"> – Tendon footprint is a curvilinear structure tapering down to the bony attachment – Look for humeral anatomic neck and beginning of articular cartilage |
| Short axis | Turn transducer 90° | Tendon is multipennate |

tendon length and is noted to be with the transducer in what would conventionally be a transverse orientation (anatomic axial plane). Hence, by turning the transducer 90° (transducer in the sagittal plane), we will be assessing the tendon in short axis. In this plane, the long head of the biceps tendon may appear as a separate round hyperechoic structure just superior to the subscapularis tendon. Given the multipennate structural arrangement of the subscapularis tendon, multiple round echogenic areas may be

seen. This is a key concept, as we do not want to misinterpret these multiple tendon slips that eventually come together to form the single conjoined tendon as it inserts on the lesser tuberosity, for a tear.

3.6.4 Step 4: Supraspinatus/Infraspinatus Tendons and Rotator Interval (Table 3.4)

There are two different ways of looking at the supraspinatus tendon, each with relative advantages. The first provides for greater hyperexten-

sion in the Crass position [9] (Fig. 3.10). The Crass position entails placing the arm behind the back with the palm pointed out. In short axis you will see the biceps tendon medially, and the supraspinatus laterally. Reorienting the transducer 90° will demonstrate the supraspinatus tendon in long axis as a convex echogenic tendon with tapering as it extends to the footprint. The second approach is a modified Crass with the difference being that the hand is placed as if it was in the back pocket [10] (Fig. 3.11). The advantage of this is less external rotation which allows for better visualization of the rotator interval. Again the biceps tendon will be located medially

Table 3.4 Supraspinatus and infraspinatus tendon imaging

| | Technique | Findings |
|----------------|--|--|
| Crass | <ul style="list-style-type: none"> – Internal rotation, hyperextension – Arm behind back, palm out, fingers toward scapula | <p>Short axis: biceps tendon medially and the supraspinatus laterally</p> <p>Long axis: supraspinatus tendon in long axis → convex echogenic tendon with tapering as it extends to the footprint</p> |
| Modified Crass | Arm behind back with hand in “back pocket” | <p>Short axis: biceps tendon medially, then the rotator interval, then the supraspinatus laterally</p> <p>Long axis: supraspinatus tendon in long axis → may see less of the tendon</p> |

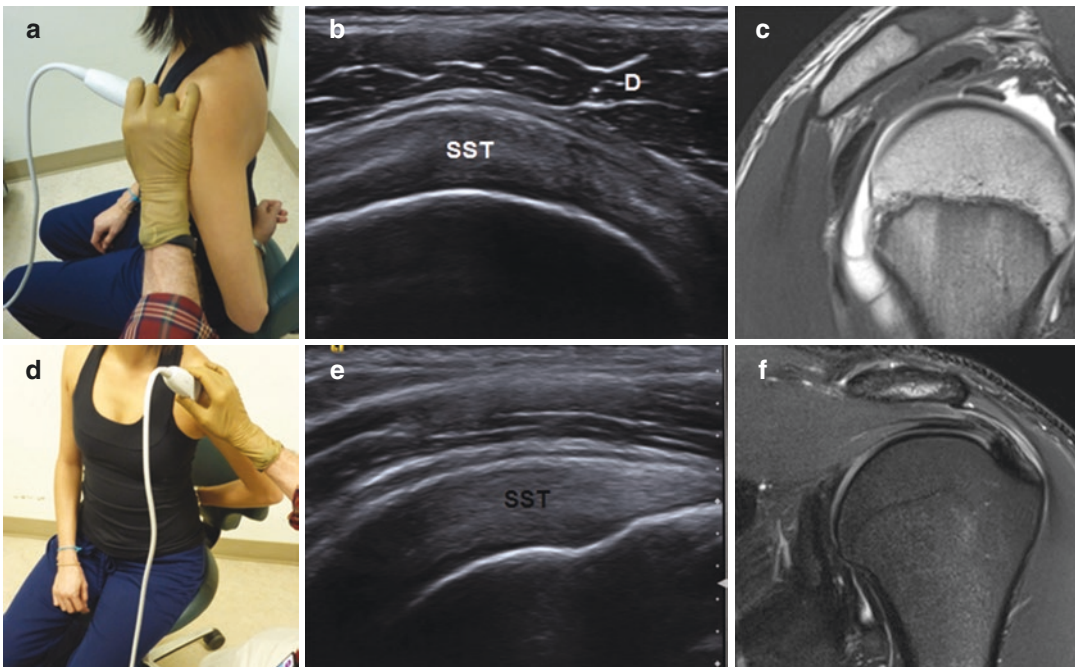


Fig. 3.10 Crass position: supraspinatus/infraspinatus and rotator interval—short-axis patient positioning (a); short-axis sonographic image (b); MR correlate of short

axis (c); long-axis patient positioning (d); long-axis sonographic image (e); MR correlate of long axis (f); supraspinatus tendon (SST); deltoid (D)

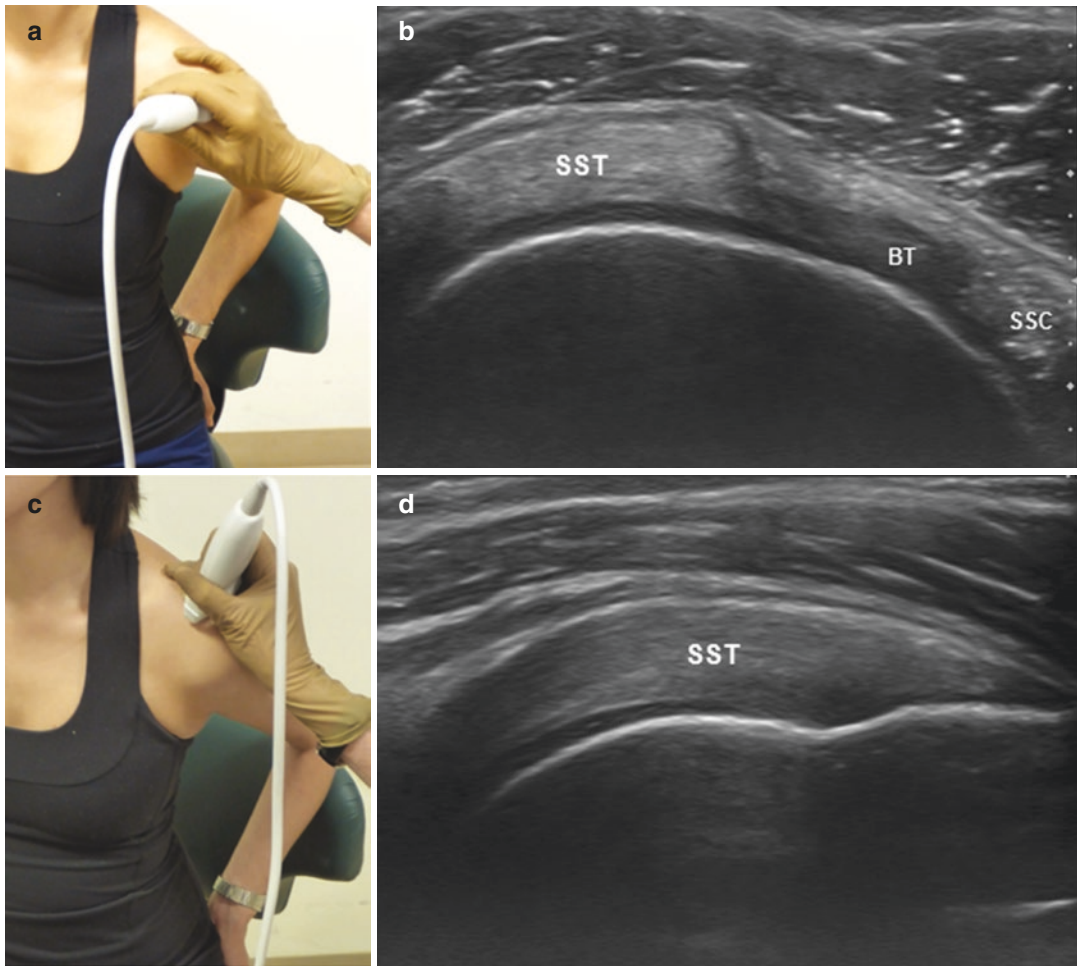


Fig. 3.11 Modified Crass supraspinatus/infraspinatus and rotator interval— short-axis patient positioning (a); short-axis sonographic image (c); long-axis patient posi-

tioning (b); long-axis sonographic image (d); supraspinatus (SST); biceps tendon (BT); subscapularis (SSC)

and the rotator interval and supraspinatus tendon laterally. The disadvantage is that you tend to not see as much of the tendon while the arm is in hyperextension. However, studies demonstrate no significant difference in the overall accuracy when comparing the two techniques [11]. If the patient can tolerate both positions we believe that there is added value in performing both with optimal visualization of both the supraspinatus tendon and the rotator interval in the modified Crass and Crass, respectively. Of note the modified Crass may be more comfortable for certain

patients, especially in cases of adhesive capsulitis.

It is important to note, particularly when scanning the rotator cuff in short axis, that there is a transitional zone where there is a blending of both infraspinatus and supraspinatus fibers (Fig. 3.12). As a rule of thumb from the level of the rotator interval approximately 2 cm from its anterior margin will be supraspinatus tendon, then there is a junctional zone with mixed supraspinatus and infraspinatus fibers, and more posteriorly there will be the infraspinatus tendon.

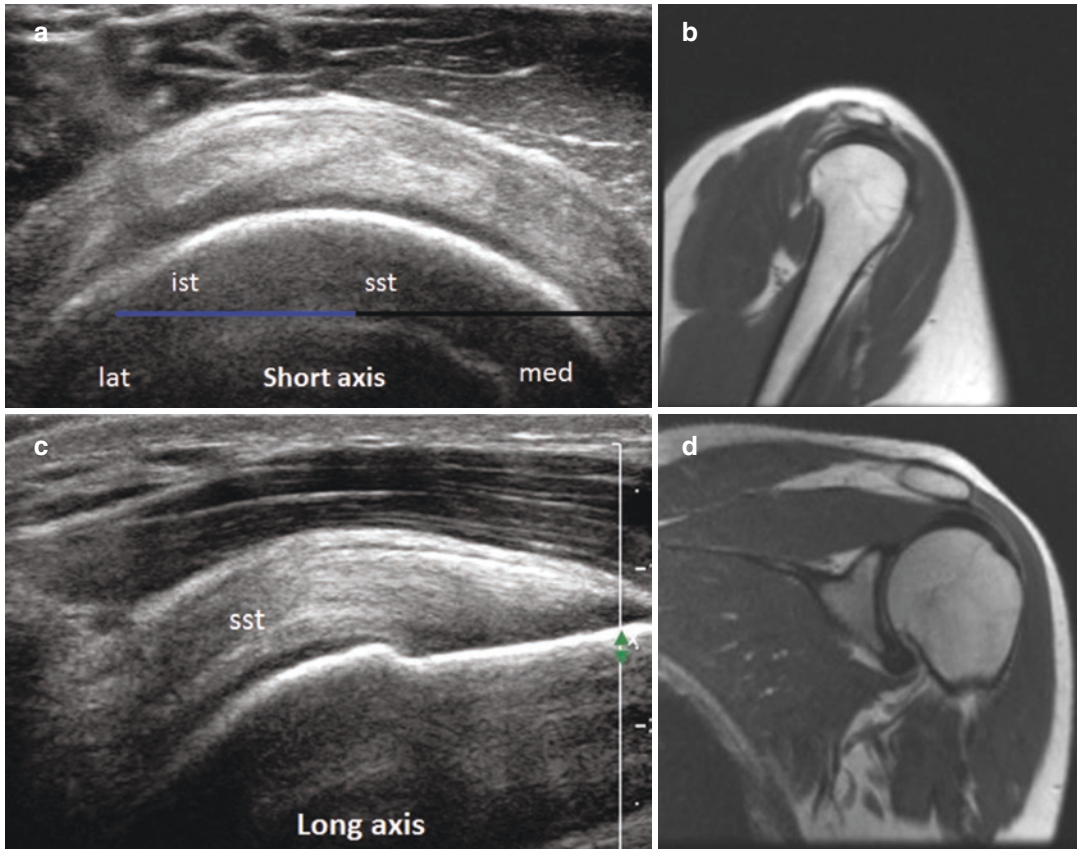


Fig. 3.12 Rotator cuff—short-axis sonographic image (a); short-axis MRI correlate (b); long-axis sonographic image (c); long-axis MRI correlate (d); supraspinatus ten-

don (SST); infraspinatus tendon (IST): In short axis generally 2 cm lateral to the rotator interval will be the supraspinatus tendon

3.6.5 Step 5: Muscle Evaluation—Supraspinatus (Fig. 3.1)

Muscle evaluation is crucial as atrophy and fatty infiltration have been shown to be associated with failed rotator cuff repairs and poor clinical outcomes [12]. Evaluation of the muscle is a fairly simple portion of the exam. Initially place the transducer in a sagittal orientation superior to the spine of the scapula to evaluate the supraspinatus muscle in the suprascapular fossa with the trapezius muscle overlying it. Again note that normal muscle is hypoechoic and within that hypoechoic background curvilinear echogenic areas are seen, corresponding to the perimysial connective tissue.

3.6.6 Step 6: Muscle Evaluation—Infraspinatus and Teres Minor (Fig. 3.2)

Position the transducer more posteriorly and caudally below the level of the scapular spine you will find the infraspinatus muscle in the infraspinatus fossa. Moving the transducer slightly caudally you will see the teres minor muscle.

Evaluation of the subscapularis muscle is limited due to the lack of a proper acoustic window, as the muscle lies deep to the pectoralis and thorax anteriorly, and the scapula posteriorly. Accounting for these limitations the muscle tissue interposed between the tendon fascicles can be imaged along the course of the multipennate

tendon insertional fibers and, as described earlier, they should not be mistaken for a tendon tear.

3.7 Conclusion

Shoulder sonography has been proven to be a sensitive and specific diagnostic tool in assessing shoulder pathology. With the implementation of a standardized protocol, such as the one outlined in this chapter, accompanied by appropriate knowledge of the sonographic shoulder anatomy we believe that it can be utilized as a powerful addition to the radiologist's armamentarium.

References

1. De Jesus JO, Parker L, Frangos AJ, Nazarian LN. Accuracy of MRI, MR arthrography, and ultrasound in the diagnosis of rotator cuff tears: a meta-analysis. *AJR Am J Roentgenol.* 2009;192(6):1701–7.
2. Le Corroller T, Cohen M, Aswad R, Pauly V, Champsaur P. Sonography of the painful shoulder: role of the operator's experience. *Skelet Radiol.* 2008;37(11):979–86.
3. Jacobson JA. Shoulder US: anatomy, technique, and scanning pitfalls. *Radiology.* 2011;260(1):6–16.
4. Minagawa H, Itoi E, Konno N, Kido T, Sano A, Uramaya M, et al. Humeral attachment of the supraspinatus and infraspinatus tendons: an anatomic study. *Arthroscopy.* 1998;14(3):302–6.
5. Crass JR, van de Vegte GL, Harkavy LA. Tendon echogenicity: ex vivo study. *Radiology.* 1988;167(2):499–501.
6. Finnoff JT, Smith J, Peck ER. Ultrasonography of the shoulder. *Phys Med Rehabil Clin N Am.* 2010;21:481–507.
7. Moosikasuwan JB, Miller TT, Burke BJ. Rotator cuff tears: clinical, radiographic, and US findings. *Radiographics.* 2005;25:1591–607.
8. Bureau NJ, Beauchamp M, Cardinal E, Brassard P. Dynamic sonography evaluation of shoulder impingement syndrome. *AJR Am J Roentgenol.* 2006;187(1):216–20.
9. Crass JR, Craig EV, Feinberg SB. The hyperextended internal rotation view in rotator cuff ultrasonography. *J Clin Ultrasound.* 1987;15(6):416–20.
10. Ferri M, Finlay K, Popowich T, Stamp G, Schuringa P, Friedman L. Sonography of full-thickness supraspinatus tears: comparison of patient positioning technique with surgical correlation. *AJR Am J Roentgenol.* 2005;184(1):180–4.
11. Shah NP, Miller TT, Stock H, Adler RS. Sonography of supraspinatus tendon abnormalities in the neutral versus crass and modified crass positions a prospective study. *J Ultrasound Med.* 2012;31(8):1203–8.
12. Kuzel BR, Grindel S, Papandrea R, Ziegler D. Fatty infiltration and rotator cuff atrophy. *J Am Acad Orthop Surg.* 2013;21(10):613–23.